Asian Journal of Chemistry; Vol. 27, No. 1 (2015), 371-374

ASIAN JOURNAL OF CHEMISTRY

http://dx.doi.org/10.14233/ajchem.2015.18385

Solvent Assisted Synthesis of Tin-Zinc Oxide Nanoparticles: Structural Characterization and Antimicrobial Activity

M. ARSHAD[1], M.A. FARRUKH[1,*], A. IMTIAZ[1] and N. NOOR[2]

[1]Department of Chemistry, Government College University, Lahore-54000, Pakistan
[2]Department of Chemistry, University of Agriculture, Faisalabad-38000, Pakistan

*Corresponding author: E-mail: akhyar100@gmail.com

Received: 30 June 2014; *Accepted*: 8 October 2014; *Published online*: 26 December 2014; AJC-16575

Tin oxide doped zinc oxide nanoparticles (SnO_2/ZnO) were prepared *via* deposition precipitation method with different molar ratios of tin oxide and effect of variation of concentrations of dopant (SnO_2) was observed for physical and chemical properties of these nanoparticle. The structural properties of nanoparticles were characterized by thermogravimetric analysis, fourier transform infrared spectrometry, powder X-ray diffraction, scanning electron microscopy and transmission electron microscopy. Their crystallite and structural properties deduced a clear decrement in crystallite size from 9.95 to 2.54 nm. Doping of tin significantly enhanced the photoluminescence and antibacterial properties of SnO_2/ZnO nanoparticles. The photoluminescence studies exhibited a strong emission of green-yellow band at 470 nm. The antibacterial activities of these nanoparticles were investigated against *Pasteurellamultocida* and *Escherichia coli* by using disc diffusion method.

Keywords: SnO_2/ZnO, Deposition precipitation, Photoluminescence, Antimicrobial activity.

INTRODUCTION

Several studies have indicated that nanoparticles can be used as efficient antibacterial agents. Metal nanoparticles like silver[1], copper[2] and iron[3] nanoparticles showed a high degree of antibacterial properties. Apart from these, metal oxide nanoparticles like magnesium oxide[4], calcium oxide[5], titanium oxide[6], tin oxide[7] and iron oxide[8] were also found effective against drug resistant bacteria.

Zinc oxide powder has been used interminably as an active constituent in ointment, creams and lotions for skin treatments owing to its antibacterial properties[9-12]. However, zinc oxide nanoparticles are much more effective in inhibition of micro-organism growth. Furthermore, at nanoscale the properties of particles are widely changed, enhancing their semiconducting abilities as well as the efficacy in inhibiting the growth of bacteria[13-15].

Nanoparticles can be synthesized by hydrothermal method[16], deposition-precipitation method[17], anodization method[18], wet oxidation[19] and sol-gel method[20], aided by surface modifiers (surfactant and solvents). The catalytic activity and antimicrobial properties of nanoparticles can be enhanced by doping the nanoparticles with metals[21]. Anti-microbial activity of zinc oxide against pathogenic organisms was increased by doping of different metals. Doped ZnO nanoparticles can potentially be antibacterial agents to treat the diseases caused by bacteria. Zinc oxide nanoparticles show semiconductor properties with wide band gap energy, which can be enhanced by doping of metals like iron, silver, cobalt and transition metals[22-25].

Tin is the semiconductor with lower band gap energy and its doping on zinc oxide nanoparticles can significantly change their optical and antibacterial properties[26,27]. In the present study, the effect of doping of tin metal on zinc oxide nano-particles is evaluated by studying their optical and antibacterial properties. For this purpose, antibacterial activity of SnO_2/ZnO nanoparticles is studied against strains of pathogenic bacteria *i.e*. *Pasteurellamultocida* and *Escherichia coli*.

EXPERIMENTAL

SnO_2/ZnO nanoparticles were synthesised by using tin chloride ($SnCl_4.5H_2O$) (Unichem), tartaric acid (Panreac), 2-propanol (Fisher), ammonia (NH_3) (Biom), sodium hydroxide (NaOH) (Merck). All the chemicals were analytical grade reagents and used without further purification.

Synthesis of SnO_2/ZnO nanoparticles: 0.35 g $SnCl_4.5H_2O$ and 0.15 g tartaric acid were added in 10 mL 2-propanol and stirred for 20 min to make homogenous mixture and volume was made up to 40 mL by adding distilled water. Zinc oxide

was added in this mixture as supporting material. 2 mL ammonia solution was added in this mixture drop by drop and pH was adjusted at 6.2. The suspension was stirred for 3 h at 70 °C and then centrifuged at 3000 rpm for 0.5 min. The precipitates were separated, washed several times with water and methanol and dried overnight at 70 °C. Finally the product was calcined at 700 °C for 4 h. SnO_2/ZnO nanoparticles with molar ratios 0.025/0.3, 0.1/0.3 and 0.05/0.3 M were prepared with same procedure.

Antibacterial activity: Antibacterial activity of SnO_2/ZnO nanoparticles were studied against two bacterial strains; *Escherichia coli* and *Pasteurellamultocida.*

Preparation of fresh bacterial culture: Nutrient broth (Oxoid, UK) 100 mL was prepared in Erlenmeyer flask contained glass beads. pH was adjusted to 7.4 by addition of buffer solution and autoclaved at 121 °C for 15 min. Mixture was allowed to cool in laminar air flow. Broth was inoculated with 100 µL bacteria form stored bacterial culture. Growth medium was incubated in shaker at 37 °C for 24 h to get 5×10^9 cells per mL[28].

Plate assay/disc diffusion method: Nutrient agar was prepared by mixing agar medium in distilled water. Agar medium and 10 mm discs of wicks paper were sterilized in autoclave and allowed to cool in laminer air flow. Cool agar medium was inoculated with 50 µL fresh bacterial culture. Sterilized discs were poured with synthesized nanoparticles and spread in petri plates with positive control in the Centre. Incubate the petri dishes at 37 °C for 24 h. Zones were measured with zone reader. Experiment was performed with both bacterial strains[28].

Spectrophotometric assay: Minimum inhibitory concentrations (MICs) were obtained by spectrophotometric assay. Nutrient broth of about 7.4 pH was prepared and autoclaved. MICs were established in round bottom 96 well micro plates. Wells of row one from A-F of plate was poured with 100 µL synthesized nanoparticles while G and H rows of 1st column were poured with water (as negative control) and standard amoxicillin (as positive control), respectively. All wells except 1st row were poured with 50 µL broth medium. Dilute each row by shifting 50 µL from 1st to 12th well and discard 50 µL from last well. Pour 10 µL of bacterial solution in all wells. Incubate for 24 h at 37 °C. Poured resazurin solution in each well and absorbance was measured at 620 nm in ELIZA microplate reader. MIC of all samples were evaluated by following formula[29].

Inhibition (%) = $(1\text{-}Ab._1/Ab._2)$

$Ab._1$ = Absorbance of sample or standard (Positive control)

$Ab._2$ = Absorbance of negative control

Crystal structure of the prepared nanoparticles was analyzed by using Philips X'pert diffractometer supplied with copper X-ray tube ($\lambda_{K\times1}$ = 1.54601Å). The morphology of nanoparticles was determined by field emission electron microscopy (FESEM) by using JEOL 7600 and Philips CM12, 80 kV, transmission electron microscope (TEM). Photoluminescence spectra was obtained by Hitachi F-7000 FL spectrophotometer. Fourier transforms infrared spectrometer (FTIR) spectrum was recorded in KBR dispersion in the range of 4000-400 cm^{-1}. Thermogravimetric analysis (TGA/DSC) of the nanoparticles were carried out by using (SDT Q 600V 8.3 Build 101).

RESULTS AND DISCUSSION

Thermogravimetric analysis: Fig. 1 shows that first weight lost occurred from 50 to 200 °C which is attributed to the loss of water and organic residue present in it. Second weight loss is due to formation of SnO_2/ZnO from $Sn(OH)_2$/ZnO with the weight loss of 22 % from 170 to 290 °C.

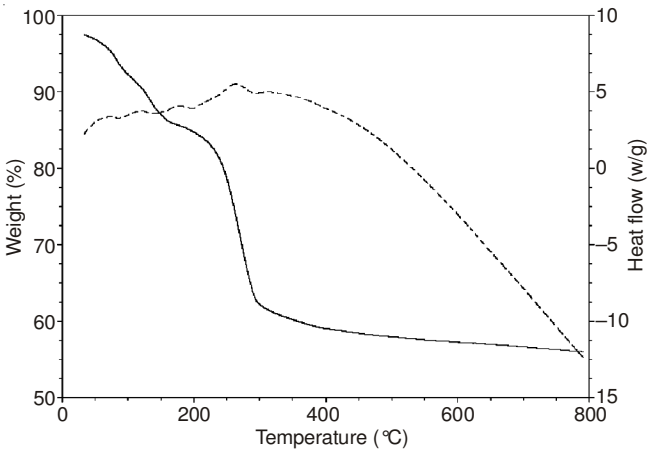

Fig. 1. TGA (solid line)/DSC (dotted line) plots of uncalcined sampleSnO_2/ZnO nanoparticles

FTIR analysis: Fig. 2 shows the FTIR spectrum SnO_2/ZnO nanoparticles at different tin metal concentrations. The peaks present in 500-450 cm^{-1} region are correlated to Zn-O bond and peaks 700-650 cm^{-1} region can be attributed to the bonding of tin with zinc oxide surface[26,30]. From the spectrum it can be seen that as the concentration of tin increases, the spectrum becomes broader. The peaks in the range of 3431 cm^{-1} represent the O-H stretching vibrations and the peaks at 2345 cm^{-1} represent the CO_2 adsorbed on the surface of nanoparticles. The peaks in the range of 1600-1400 cm^{-1} correspond to the C=O bonds. The adsorbed bands at 1633 cm^{-1} assigned to O-H bonding vibration which is becoming broad as the concentration is increasing[31].

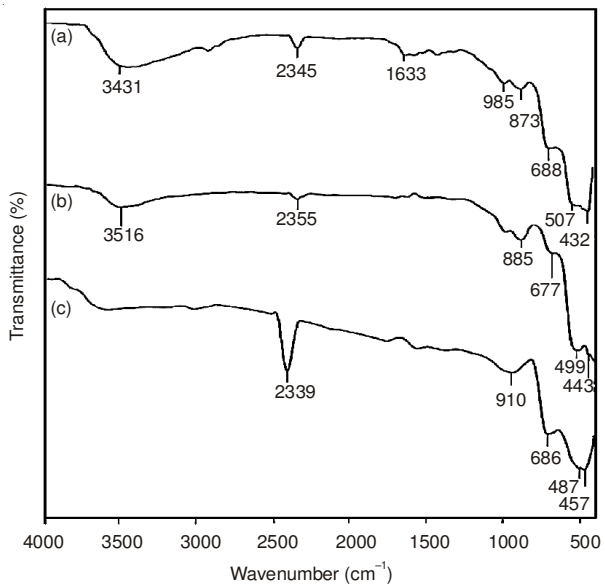

Fig. 2. FTIR spectra for (a) 0.025/0.3, (b) 0.1/0.3 and (c) 0.05/0.3 SnO_2/ZnO nanoparticles

X-ray powder diffraction analysis: The lattice parameters of tin doped zinc oxide nanoparticles are well agreed with the ICCD PDF database. The essential peaks of zinc oxide nanoparticles are present at 2θ = 31.81° (100), 34.46° (002), 36.22° (101), 47.9° (012), 56.41° (110), 62.83° (013), 66.34° (200), 67.89° (112) which are all well indexed with the PDF #01-089-0510. The results show a typical hexagonal wurtize structure of zinc oxide (Fig. 3). In addition to zinc oxide peaks, few weak peaks of tin oxide with tetragonal structure at 2θ = 26.5° (110), 33.87° (101) and 51.6° (211) also have been observed (PDF # 00-003-1114).

X-ray powder diffraction peaks showed that upon increasing tin metal dopant concentration, the intensity of the corresponding peak towards the planes (002) is found to decrease and intensity of peaks towards the planes (100) and (101) increases.

According to modified Scherrer's equation

$$D = \frac{k\lambda}{\beta(\cos\theta)} \quad (1)$$

D is the average crystallite size, β is the broadening of peak at half the maximum intensity in radians. λ wavelength of incident radiations in nm, k is the grain shape dependant constant (k = 0.89) and θ is diffraction angle. Average crystallite size for SnO_2/ZnO nanoparticles with molar ratios 0.025/0.3, 0.1/0.3 and 0.05/0.3 were 9.95, 8.7, 2.54 nm, respectively[2] (Fig. 3).

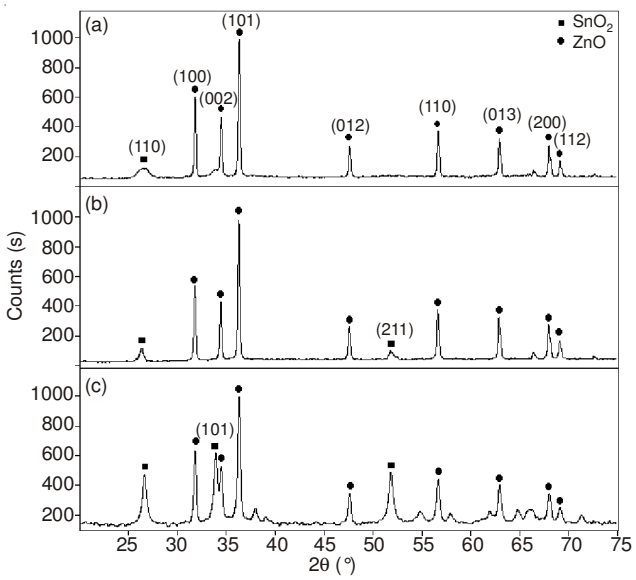

Fig. 3. XRD spectra for (a) 0.025/0.3 M, (b) 0.1/0.3 M and (c) 0.05/0.3 M SnO_2/ZnO nanoparticles

FESEM of SnO_2/ZnO nanoparticles: FESEM images of SnO_2/ZnO nanoparticles are shown in Fig. 4. The shape of 0.025/0.3 SnO_2 nanoparticles looks like rice. As molar concentration of SnO_2 is increasing, the morphology of nano-sized particle is changing from rice like to diamond like structure. When the concentration of tin metal is low, particles are more easily agglomerate with each other. As concentration is increasing the structure of particles is changing.

TEM of SnO_2/ZnO nanoparticles: Fig. 5 shows the TEM image of SnO_2/ZnO nanoparticles exhibits aggregated nanoparticles which form a spindle shaped morphology in which there are some black spots which indicate the presence of SnO_2 with an average diameter of about 7.57 nm.

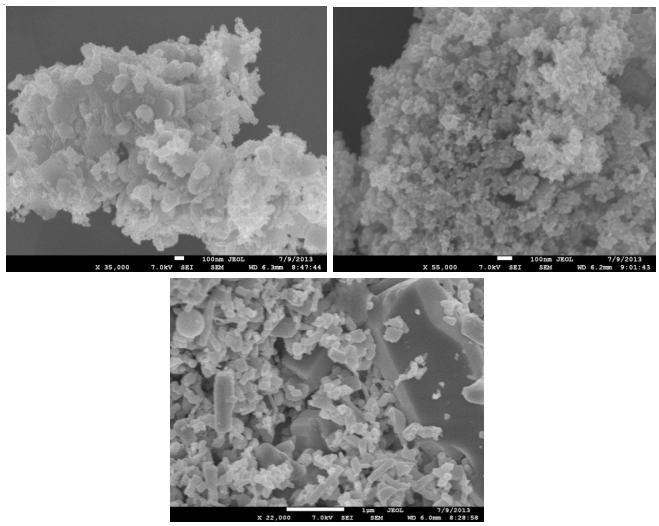

Fig. 4. FESEM images for (a) 0.025/0.3, (b) 0.1/0.3 and (c) 0.05/0.3 M SnO_2/ZnO nanoparticles

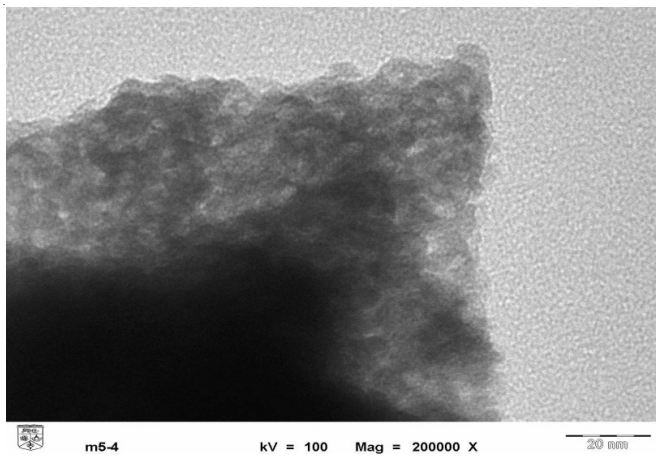

Fig. 5. TEM image of SnO_2/ZnO nanoparticles

Photoluminescence spectroscopy of SnO_2/ZnO nanopaticles: Fig. 6 Shows the photoluminescence spectra of SnO_2/ZnO nanoparticles at different molar ratios (0.025/0.3, 0.1/0.3 and 0.05/0.3). All the samples show two distinct emission peaks sharp, one in UV region and other broad in visible green region. Zinc oxide give peak at 420 and 480 nm and a broad peak around 450 nm can be attributed to the tin oxide[32,33]. With

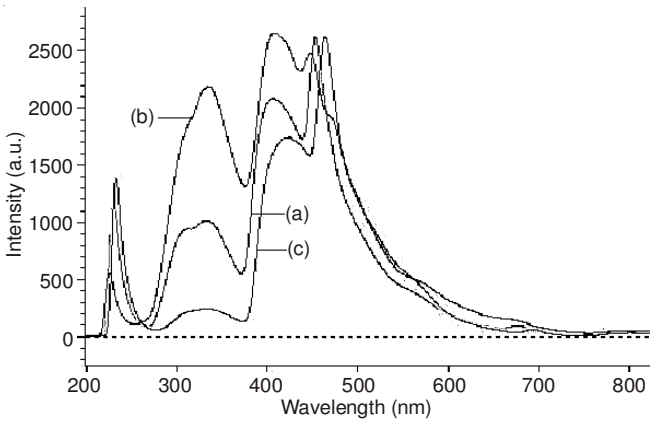

Fig. 6. Photoluminescence spectra for (a) 0.025/0.3, (b) 0.1/0.3 and (c) 0.05/0.3 SnO_2/ZnO nanoparticles

the increase in concentration of dopant tin oxide, the intensity of its corresponding peak increases. Blue shift is observed, which may be due to the modulation of band gap caused by dopant tin oxide. Blue green emission band results from the recombination of singly ionized oxygen vacancy of zinc oxide and photogenerated hole[34].

Antimicrobial activity: Antimicrobial activities of nanoparticles are given in the Fig. 7 has shown maximum inhibition against both tested strains followed by 0.05 SnO_2/0.3 ZnO nanoparticles with while minimum inhibition was shown by 0.025 SnO_2/0.3 ZnO nanoparticles.

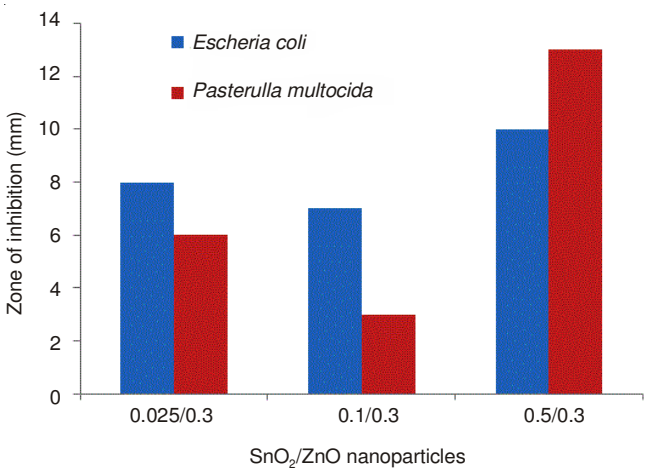

Fig. 7. Antimicrobial activity of SnO_2/ZnO nanoparticles

Minimum inhibitory concentration: Minimum inhibitory concentrations of samples are given in Table-1. SnO_2/ZnO nanoparticles with molar ratio 0.05/0.3 have been found to inhibit the *Escherichia coli* and *Pasteurellamultocida* at very low concentrations, 0.025 and 0.019 mg/mL, respectively. While highest concentrations of SnO_2/ZnO with molar ratio 0.025/0.3 nanoparticles required for inhibition of both microbes, 0.15 and 0.312 mg/mL, respectively.

TABLE-1
MINIMUM INHIBITORY CONCENTRATION OF SnO_2/ZnO NANOPARTICLES AGAINST *Escherichia coli* AND *Pasteurellamultocida*

Sample	*Escherichia coli* (mg/mL)	*Pasteurellamultocida* (mg/mL)
0.02 SnO_2/0.3 ZnO	0.150	0.312
0.10 SnO_2/0.3 ZnO	0.780	1.250
0.05 SnO_2/0.3 ZnO	0.025	0.019
Standard (Amoxicillin)	0.004	0.004

Conclusion

SnO_2/ZnO nanoparticles were synthesized using deposition-precipitation method with various concentration of tin metal ion. It was observed that the activities of nanoparticles against bacterial strains are directly related with the concentration of tin metal ion doped on zinc oxide nanoparticles. SnO_2/ZnO nanoparticles with 0.05/0.3 molar ratio showed maximum activity against the bacterial strains followed by 0.1/0.3 and 0.025/0.3 molar ratios. It was observed that growth inhibition of the *Pasteurellamultocida* was less at very low concentration of dopant tin metal, while high concentration of dopant tin favours high inhibition growth of both microbial strains. The zone of inhibition developed by 0.05/0.3 SnO_2/ZnO nanoparticles against *Escherichia coli* is 0.025 mg/mL followed by 0.025/0.3 and 0.1/0.3 molar ratios of SnO_2/ZnO nanoparticles which is 0.15 and 0.78 mg/mL, respectively. In the same way, zone of inhibition developed by 0.05/0.3 SnO_2/ZnO nanoparticles against *Pasteurellamultocida* is 0.019 mg/mL which is less than 0.1/0.3 and 0.025/0.3 SnO_2/ZnO nanoparticles (1.25 and 0.312 mg/mL, respectively). It was observed that 0.05/0.3 SnO_2/ZnO nanoparticles with smallest particle size exhibit high antimicrobial potential by both the assays, while 0.1/0.3 and 0.05/0.3 SnO_2/ZnO nanoparticles have minimum inhibitory potential determined by both the assays.

REFERENCES

1. I. Sondi and B. Salopek-Sondi, *J. Colloid Interf. Sci.*, **275**, 177 (2004).
2. J.P. Ruparelia, A.K. Chatterjee, S.P. Duttagupta and S. Mukherji, *Acta Biomater.*, **4**, 707 (2008).
3. C. Lee, J.Y. Kim, W.I. Lee, K.L. Nelson, J. Yoon and D.L. Sedlak, *Environ. Sci. Technol.*, **42**, 4927 (2008).
4. P.K. Stoimenov, R.L. Klinger, G.L. Marchin and K.J. Klabunde, *Langmuir*, **18**, 6679 (2002).
5. A. Roy, S.S. Gauri, M. Bhattacharya and J. Bhattacharya, *J. Biomed. Nanotechnol.*, **9**, 1570 (2013).
6. H. Foster, I. Ditta, S. Varghese and A. Steele, *Appl. Microbiol. Biotechnol.*, **90**, 1847 (2011).
7. C. Karunakaran, S. Sakthi Raadha and P. Gomathisankar, *J. Alloys Comp.*, **549**, 269 (2013).
8. N. Tran, A. Mir, D. Mallik, A. Sinha, S. Nayar and T.J. Webster, *Int. J. Nanomedicine*, **5**, 277 (2010).
9. A.K. Gupta and A.R. Skinner, *Int. J. Dermatol.*, **43**, 830 (2004).
10. W.R. Moorer and J.M. Genet, *Oral Surg. Oral Med. Oral Pathol. Oral Radiol. Endod.*, **53**, 508 (1982).
11. H.R. Godfrey, N.J. Godfrey, J.C. Godfrey and D. Riley, *Altern. Ther. Health Med.*, **7**, 49 (2001).
12. Papageorgiou and Chu, *Clin. Exp. Dermatol.*, **25**, 16 (2000).
13. N. Jones, B. Ray, K.T. Ranjit and A.C. Manna, *FEMS Microbiol. Lett.*, **279**, 71 (2008).
14. L.C. Ann, S. Mahmud, S.K.M. Bakhori, A. Sirelkhatim, D. Mohamad, H. Hasan, A. Seeni and R.A. Rahman, *Ceram. Int.*, **40**, 2993 (2014).
15. K.R. Raghupathi, R.T. Koodali and A.C. Manna, *Langmuir*, **27**, 4020 (2011).
16. S. Ali, M.A. Farrukh and M. Khaleeq-ur-Rahman, *Korean J. Chem. Eng.*, **30**, 2100 (2013).
17. A. Imtiaz, M.A. Farrukh, M. Khaleeq-ur-Rahman, R. Adnan, *The Scientific World J.*, 2013 (2013).
18. G. Huey-Shya, R. Adnan and M.A. Farrukh, *Turk. J. Chem.*, **35**, 375 (2011).
19. K.M.A. Saron, M.R. Hashim and M.A. Farrukh, *Appl. Surf. Sci.*, **258**, 5200 (2012).
20. R. Adnan, N.A. Razana, I.A. Rahman and M.A. Farrukh, *J. Chil. Chem. Soc.*, **57**, 222 (2010).
21. R.K. Dutta, B.P. Nenavathu and S. Talukdar, *Colloids Surf. B*, **114**, 218 (2014).
22. M.G. Nair, M. Nirmala, K. Rekha and A. Anukaliani, *Mater. Lett.*, **65**, 1797 (2011).
23. R.K. Dutta, P.K. Sharma, R. Bhargava, N. Kumar and A.C. Pandey, *J. Phys. Chem. B*, **114**, 5594 (2010).
24. M. Li, S. Pokhrel, X. Jin, L. Mädler, R. Damoiseaux and E.M.V. Hoek, *Environ. Sci. Technol.*, **45**, 755 (2011).
25. T. Jan, J. Iqbal, M. Ismail and A. Mahmood, *J. Appl. Phys.*, 115, 154308 (2014).
26. J.I. Tariq Jan, M. Ismail, M. Zakaullah, S.H. Naqvi and N. Badshah, *Int. J. Nanomed.*, **8**, 3679 (2013).
27. S. Ameen, M.S. Akhtar, H.-K. Seo, Y.S. Kim and H.S. Shin, *Chem. Eng. J.*, **187**, 351 (2012).
28. H. Meruvu, M. Vangalapati, S.C. Chippada and S.R. Bammidi, *J. Rasayan Chem.*, **4**, 217 (2011).
29. B. Stephen Inbaraj, T.-Y. Tsai and B.-H. Chen, *Sci. Technol. Adv. Mater.*, **13**, 15002 (2012).
30. M.A. Farrukh, B.-T. Heng and R. Adnan, *Turk. J. Chem.*, **34**, 537 (2010).
31. S. Tanveer, M.A. Farrukh, S. Ali, M. Khaleeq-ur-Rahman and A. Imtiaz, *J. Chin. Chem. Soc.*, **61**, 525 (2014).
32. V. Kuzhalosai, B. Subash, A. Senthilraja, P. Dhatshanamurthi and M. Shanthi, *Spectrochim. Acta A*, **115**, 876 (2013).
33. J. Dai, C. Xu, J. Guo, X. Xu, G. Zhu and Y. Lin, *AIP Advanc.*, 3, (2013).
34. E. Kowsari and M.R. Ghezelbash, *Mater. Lett.*, **68**, 17 (2012).